



Classification of auxin plant hormones by interaction property similarity indices

Sanja Tomić^{a,b}, Razif R. Gabdoulline^a, Biserka Kojić-Prodić^b & Rebecca C. Wade^{a,*}

^a*European Molecular Biology Laboratory, Meyerhofstrasse 1, D-69117 Heidelberg, Germany*

^b*Ruđer Bošković Institute, P.O. Box 1016, HR-10001 Zagreb, Croatia*

Received 16 May 1997; Accepted 20 August 1997

Key words: auxins, molecular alignment, molecular interaction field, molecular modeling, QSAR, similarity index

Summary

Although auxins were the first type of plant hormone to be identified, little is known about the molecular mechanism of this important class of plant hormones. We present a classification of a set of about 50 compounds with measured auxin activities, according to their interaction properties. Four classes of compounds were defined: strongly active, weakly active with weak antiauxin behaviour, inactive and inhibitory. All compounds were modeled in two low-energy conformations, 'P' and 'T', so as to obtain the best match to the 'planar' and 'tilted' conformations, respectively, of indole 3-acetic acid. Each set of conformers was superimposed separately using several different alignment schemes. Molecular interaction energy fields were computed for each molecule with five different chemical probes and then compared by computing similarity indices. Similarity analysis showed that the classes are on average distinguishable, with better differentiation achieved for the T conformers than the P conformers. This indicates that the T conformation might be the active one. Further, a screening was developed which could distinguish compounds with auxin activity from inactive compounds and most antiauxins using the T conformers. The classifications rationalize ambiguities in activity data found in the literature and should be of value in predicting the activities of new plant growth substances and herbicides.

Introduction

Plant hormones, also known as phytohormones or plant growth substances, are naturally occurring substances which, in low concentrations, influence plant physiology. The term plant growth regulators, although also used for plant hormones, encompasses all compounds, natural and synthetic, which when applied to plants evoke a specific physiological response. Of the five groups of plant hormones, the auxins are dealt with in the present analysis. Auxins promote cell enlargement and division, apical dominance, root initiation, differentiation of vascular tissue, signaling, and other activities [1]. However, little is known of their activity at the molecular level [1–5]. They belong to a chemically diverse class of compounds, most of which have an aromatic system such as indole, phenyl or

naphthalene with a side chain containing a carboxyl group attached. Indole-3-acetic acid (IAA) is the most commonly occurring natural auxin, and is followed by 4-chlorindole-3-acetic acid and phenylacetic acid whose distribution is more restricted [1,2]. There are many synthetic auxins and some of them, e.g. 2,4-dichlorophenoxyacetic acid, are used agriculturally as growth regulators and herbicides.

The auxin receptor and auxin binding proteins have been central elements in most hypotheses aiming to explain phytohormone action at a molecular level [1–12]. A number of auxin binding proteins (ABPs) have been detected during an almost two-decade long search for such proteins [1–12 and references therein]. Among them, the maize ABP1, a homodimer of 22-kDa subunits, is the clearest candidate for an auxin receptor [1–12]. This protein is located mainly within the lumen of the endoplasmic reticulum, but an important fraction appears to function on the outside

*To whom correspondence should be addressed.

of the plasma membrane. A three-dimensional structure of ABP1 would provide a basis for understanding the auxin binding mechanism and rationally designing new substrate analogues (growth regulators) or inhibitors (e.g. herbicides). However, this approach is not possible because no 3D structure has yet been solved and there is insufficient data for homology modeling of the ABP1.

Thus, in auxin activity studies, the focus has been on analysis of the ligands, mostly by evaluation of their charge distributions and conformations [13–29]. The seminal hypotheses for how auxins bind to the receptor's active site and induce a response are: (1) the requirement for a specified charge separation distance in the auxins introduced by Porter and Thimann [14] and later modified by Farrimond et al. [16]; (2) the conformational change of the auxin from a planar recognition conformation to a tilted modulation conformation on binding to the active site introduced by Kaethner [15]; and (3) the receptor topography hypothesis introduced by Katekar [19] and Rakhminova et al. [18], requiring complementarity of the binding site and ligand, based on analysis of shape, size, lipophilicity and the orientation of the active groups.

So far, however, a systematic classification of compounds for auxin activity based on molecular properties has not been performed. This is the aim of this paper, in which we show how similarity calculations can be used as a tool for rationalizing ambiguities regarding biological data and generating a model for predicting the activity of potential auxins and anti-auxins. Auxin compounds are divided into classes according to their measured biological activity and the similarity calculated between compounds and classes of compounds. This requires modeling of the compounds (conformational analysis and energetic evaluation of conformers), molecular alignment, calculation of their interaction energies with selected chemical probes, molecular interaction fields (MIFs) [30], and then computation of similarity indices for the MIFs. Similarity indices (SIs) have long been used to compare electron densities and potentials derived from quantum mechanical (QM) calculations in order to derive structure–activity relationships (SARs) [31–35]. Here we use them to compare MIFs and then to group compounds into classes accordingly. We have employed this classification rather than a more conventional analysis method, such as comparative molecular field analysis (CoMFA) [36], because of the approximate nature of the experimental activity data. Although some receptor binding data are available,

activities have mostly been measured in *in vivo* plant growth experiments. Thus, the model cannot be overly quantitative and must be reasonably robust to the variations, and sometimes inconsistencies, in activities recorded in these experiments.

A major issue in any 3D QSAR study is the alignment of the compounds. We used two approaches, one based on atomic properties, and the other on MIFs of the compounds. For the former, we used the implementation in the SEAL program by Kearsley and Smith [37]. For the latter, we developed an alignment program utilizing MIFs computed on the probe accessible surfaces of the molecules. This method is somewhat similar to the approach of Bagdassarian et al. [38], but differs in the type of property on which alignment is based and the surface used: they used an electrostatic potential derived from QM calculations on van der Waals surfaces.

The analysis consisted of two stages: initial classification and final refinement of the classification. In the first stage, molecules were aligned using the SEAL program and SIs [34, 39–41] were computed for the MIFs in a volume around each molecule. In the second stage, the similarity of MIFs computed on the molecular probe accessible surfaces was used for both alignment and classification of the molecules. The latter method resulted in higher SIs and was used to tune the initial classification and to classify additional compounds. Four classes of compounds are identified in the final model, which can be used to distinguish auxins from inactive compounds and most antiauxins.

Materials and methods

Experimental data

As shown in Table 1, compounds belonging to diverse chemical groups were analyzed: derivatives of indole-3-acetic acid (IAA), phenoxy acetic acid (PAA), phenoxy-2-propionic acid (PA2PA), benzoic acid (BA), 3-indole-3-butyric acid (3-IBA), 2-indole-3-butyric acid (i.e. indole-3-isobutyric acid, IIBA), phenoxy-isobutyric acid (PIBA) and naphthalene acetic acid (NAA). 3-Indole-3-propionic acid (3-IPA), 4-indole-3-butyric acid (4-IBA) and β -naphthoic acid were also analyzed.

Biological activity and binding measurements from the literature were used [14,20,22–25,29,42–63]. Experiments performed on *Avena* and *Mais* (monocotil plants) were chosen as the main sources of data,

Table 1. Compounds analysed and their classification

Code ^a	Compound ^b	Class		References ^c
		Final ^c	Initial ^d	
1	1-NAA	1		42, 43, 48
2* ^f	2-Me,4-Cl-PAA	1		42
3	2,5-Cl ₂ -PAA	1		42, 50
4	2,4-Cl ₂ -PAA	1		42, 43, 57, 50
5	2,5-Cl ₂ -PA2PA (R)	1		42
6	2,4-Cl ₂ -PA2PA (R and S)	1		42
7	IAA	1		42–57
8*	4-Cl-IAA	1		43, 46, 49, 57
9	5-Cl-IAA	1		47, 49, 57
10	6-Cl-IAA	1		47, 49, 57
11	5,6-Cl ₂ -IAA	1		43
12	6-F-IAA	1		24, 49
13	4-F-IAA	1		24, 49
14	4-Me-IAA	1		29, 48
15	2,3,4-Cl ₃ -PAA	1		50, 51
16	5-F-IAA	1		24, 47, 49, 63
17	4-Et-IAA	1		22, 29, 48
18	5-Me-IAA	1		22, 54
19	7-F-IAA	1		24, 49
20	4,6-Cl ₂ -IAA	1		43, 46, 47
21	2,4,5-Cl ₃ -PAA	1		50, 51, 55
22	6,7-Cl ₂ -IAA	1		43, 46, 47, 57
23	4-IBA	1		42, 45
24	2,5-Me ₂ -PA2PA (R)	1	2	42
25	7-Cl-IAA	2	1	29, 43, 46, 49, 57, 63
26*	4,7-Cl ₂ -IAA	2		29, 43, 46, 57
27*	3-IPA	2		42, 45
28	5,7-Cl ₂ -IAA	2		43, 44, 46, 57, 63
29	2-NAA	2	4	42, 59
30	2-Cl-BA	3		42
31	2-F-BA	3		55
32	2-I-BA	3		55
33	2,6-Cl ₂ -BA	3		42
34*	BA	3		42
35	4-Cl-BA	3		42
36	β-Naphtoic acid	3		52
37	2-Me-BA	3		55
38*	4-Cl-PIBA	4		42
39	IIBA	4		42
40*	5,7-Cl ₂ -IIBA	4		44
41	TFIBA (R and S)	4		45
42	3-IBA (R and S)	4		45
43	2,4-Cl ₂ -PIBA	4		44, 53
44	3,4,5-I ₃ -BA	4		42
45	3,4-Cl ₂ -BA	3, 4		42
46	2-Me-IAA	1		14, 48, 55, 63
47	2,5-Me ₂ -PAA	2		42, 55

Table 1. (continued)

Code ^a	Compound ^b	Class		References ^c
		Final ^c	Initial ^d	
48	2,3,5-Cl ₃ -BA	3		60
49	2,4,6-Cl ₃ -PAA	3, 4		50, 51, 55
50	2,3,5-I ₃ -BA	4		42, 44, 55
51	PAA	3		42, 51, 55
52	3,5-Cl ₂ -PA2PA (R and S)	4		20, 62
53	2,5-Me ₂ -PA2PA (S)	2		42

^a The compound identifier number, see Figure 1.

^b NAA: naphthalene acetic acid; PAA: phenoxy acetic acid; PA2PA: phenoxy-2-propionic acid; IAA: indole-3-acetic acid; BA: benzoic acid; 3-IPA: 3-indole-3-propionic acid; PIBA: phenoxy isobutyric acid; 4-IBA: 4-indole-3-butyric acid; 3-IBA: 3-indole-3-butyric acid; IIBA: 2-indole-3-butyric acid (indole-3-isobutyric acid); TFIBA: 4,4,4-trifluoro-3-indole-3-butyric acid.

^c Classification of compounds as a result of the final similarity analysis. Two classes are given when unambiguous classification could not be made; 1: compounds active over a wide range of concentrations (10^{-8} – 10^{-4} M); 2: very low activity compounds with antiauxin characteristics measured; 3: compounds with very low binding constants [42], inactive over a wide range of concentrations, i.e. their activity is below 0.1 IAA activity; 4: antiauxins, i.e. compounds with inhibitory characteristics, for details see the text.

^d Initial division of compounds into classes according to their measured activities and similarity between their MIFs. The initial class was the same as the final class unless a number is given. Compounds **44–53** were only introduced in the final analysis. For most of them data in the literature are incomplete or contradictory. Similarity analysis assisted in resolving the ambiguities in the literature and proper classification of these compounds.

^e References for experimental activity measurements.

^f The compounds labeled by * were used for the definition of class-kernels.

but some results from measurements on pea and oat coleoptil section were also included in the analysis. As measurements were not performed for all compounds with the same plants under the same conditions, activities were compared by computing the activity of each compound relative to IAA under the same experimental conditions.

After considering several different classifications, 46 compounds, including both stereo isomers of three compounds (Table 1, compounds **1–43**), were assigned to four classes as shown in Table 1, based on the experimental activity data and the results of similarity index analysis (see below). The compounds in class 1 are active over a wide range of concentrations (10^{-8} – 10^{-4} M). Class 2 consists of compounds of very low activity, which at certain concentrations, differing from compound to compound, show weak antiauxin behaviour [29,42–46,49,57,59,63]. The inactive compounds, class 3, have very low binding

constants [42] and are inactive over a wide range of concentrations [42,52,55]; i.e. their activity is below 0.1 [0.0 ± 0.1] IAA activity. Class 4 consists of antiauxins, i.e. compounds with inhibitory characteristics [42,44,45]. They bind strongly but produce no biological response characteristic for auxins. There are some compounds in this class for which binding data are not available (**40–43**, Table 1), but according to in vivo measurements [44,45] they are antiauxins. That is, they suppress development of tissues in which auxins, at the same concentrations, act as promoters. In addition, they enhance development of roots which auxins normally, in concentrations $\lesssim 10^{-5}$ M, do not affect.

Compounds **44–53** (Table 1) were added to the data set after the initial analysis to assign the classes. Some of these compounds are incompletely defined with regard to their biological activity, e.g. compounds **48**, **49** and **52** (Table 1) have been declared as inactive

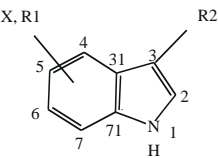
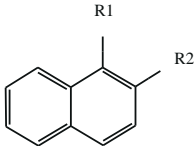
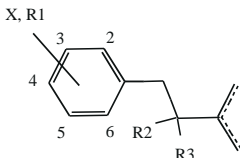
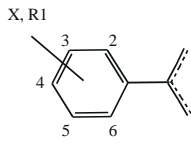
	X	R1	R2	Compounds	
	-	-	CH ₂ COO ⁻	IAA (7)	
	Cl	-	CH ₂ COO ⁻	4-Cl-IAA (8), 5-Cl-IAA (9), 6-Cl-IAA (10), 5,6-Cl ₂ -IAA (11), 4,6-Cl ₂ -IAA (20), 6,7-Cl ₂ -IAA (22), 7-Cl-IAA (25), 4,7-Cl ₂ -IAA (26), 5,7-Cl ₂ -IAA (28)	
	F	-	CH ₂ COO ⁻	6-F-IAA (12), 4-F-IAA (13), 5-F-IAA (16), 7-F-IAA (19)	
	-	CH ₃	CH ₂ COO ⁻	4-Me-IAA (14), 5-Me-IAA (18), 2-Me-IAA (46)	
	-	CH ₂ CH ₃	CH ₂ COO ⁻	4-Et-IAA (17)	
	-	-	CH ₂ CH ₂ CH ₂ COO ⁻	4-IBA (23)	
	-	-	C(CH ₃) ₂ COO ⁻	IIBA (39)	
	Cl	-	C(CH ₃) ₂ COO ⁻	5,7-Cl ₂ -IIBA (40)	
			CH ₂ CH ₂ COO ⁻ CH(CH ₃)CH ₂ COO ⁻ CH(CF ₃)CH ₂ COO ⁻	3-IPA(27) 3-IBA (R & S)(42) TFIBA (R & S)(41)	
	R1	R2			
	CH ₂ COO ⁻	H		1-NAA(1)	
	H	CH ₂ COO ⁻		2-NAA(29)	
	H	COO ⁻		β-Naphtoic acid (36)	
	X	R1	R2	R3	
	-	-	H	H	PAA(51)
	Cl	CH ₃	H	H	2-Me, 4-Cl-PAA(2)
	Cl	-	H	H	2,5-Cl ₂ -PAA(3), 2,4-Cl ₂ -PAA(4), 2,3,4-Cl ₃ -PAA(15), 2,4,5-Cl ₃ -PAA(21), 2,4,6-Cl ₃ -PAA(49)
	-	CH ₃	H	H	2,5-Me ₂ -PAA(47)
	Cl	-	CH ₃	H	2,5-Cl ₂ -PA2PA (R)(5), 2,4-Cl ₂ -PA2PA (R & S)(6), 3,5-Cl ₂ -PA2PA (R & S)(52)
	-	CH ₃	CH ₃	H	2,5-Me ₂ -PA2PA(R:24, S:53)
	Cl	-	CH ₃	CH ₃	4-Cl-PIBA(38), 2,4-Cl ₂ -PIBA(43)
	X	R1			
	-	-			BA(34)
	Cl	-			2-Cl-BA(30), 2,6-Cl ₂ -BA(33), 4-Cl-BA(35), 3,4-Cl ₂ -BA(45), 2,3,5-Cl ₃ -BA(48)
	F	-			2-F-BA(31)
	I	-			2-I-BA(32), 3,4,5-I ₃ -BA(44), 2,3,5-I ₃ -BA(50)
	-	CH ₃			2-Me-BA(37)

Figure 1. Schematic representation of the compounds modeled. The identifier codes correspond to those in Table 1.

[20,50,51,55,60], but binding tests and experiments on root development have not been published for them. Thus, it is not clear if these compounds are actually inactive or antiauxins. Some of the other compounds from this set were not included in the initial analysis because of contradictions in the literature regarding their biological activity, e.g. 2,3,5-I₃-BA is declared to be an auxin [42,55] and also an inhibitor [42,44]. Therefore, compounds **44–53** (Table 1) were analyzed to test the model and to rationalize the available activity data.

Modeling of molecular structures

Three-dimensional structures of the two low-energy conformers of each compound (see Table 1 and Figure 1) were modeled. IAA was used as the parent compound because it is the most widespread auxin and detailed *ab initio* conformational analysis has been performed for it [27,28]. The choice of IAA conformers is based on the results of *ab initio* calculations and existing theories dealing with auxin activity, which are (Figure 2): (1) the extended planar conformation with the side chain approximately in the plane of the ring and the carboxyl oxygens astride the plane; (2) the tilted conformation with the side chain pointing out of the ring plane and the carboxyl group oriented approximately perpendicular to the first side chain bond (Figure 2). This is the second lowest IAA minimum determined by *ab initio* calculations on protonated compounds [27,28] and similar results are obtained for anions (S. Tomić, M. Ramek and B. Kojić-Prodić, unpublished data).

The two conformers of all the other compounds were modeled using the INSIGHT program [64] to superimpose as closely as possible on these two IAA conformers. At the same time, they were required to preserve planarity of the aromatic ring systems that bind to the so-called ‘naphthalene binding platform’ which is, according to Rakhminova et al. [18], one of the three auxin binding regions. The set of conformers fitted to the more extended planar IAA conformer were designated ‘P’, while those fitted to the tilted conformer were designated ‘T’ (see Figure 2). As the rotational barrier for the carboxyl group is low (about a few kT at room temperature), there are other low-energy conformations. However, our choice based on QM energy profiles of IAA and some of its derivatives permits hypotheses on auxin binding to be evaluated and enables the best alignment within a set of compounds diverse in size and chemical characteristics.

Geometry optimisation of the compounds was performed with the DISCOVER program [65] using the CFF91 force field [66]. Although our previous study [27,28] on IAA and 4-Cl-IAA showed that none of the force fields tested was able to reproduce the *ab initio* potential energy surfaces (PES), a later version of the CFF91 force field (incorporated into DISCOVER, v. 2.97) turned out to give quite reliable results for the IAA anion and some IAA derivatives with propionic and isobutyric acid [79] as well as for some other conjugated systems [67]. A combined steepest descent and conjugate gradients optimization protocol was utilized until a final energy derivative ≤ 0.1 kcal/mol/Å was achieved. The conformers with relative energies within 5 kcal/mol were used for further analysis.

The transition from the P to the T conformer and *vice versa* occurs mainly by rotation about the first and the second side chain bond (Figure 2). The transition barrier between these two conformers was determined for at least one compound from each chemically different group (a few examples are given in Figure 2).

Alignment

Two alignment methods were used. The first, based on atomic properties, was used to achieve classification of auxins and their analogues. The second, based on optimizing the similarity of MIFs was used to evaluate the initial classification and derive a final classification.

Alignment based on atomic properties

The optimized conformers were aligned using the SEAL program [37]. Partial atomic charges from the CVFF parameter set [68] were used. It was found that these charges are in good agreement ($R \approx 0.98$) with charges determined from Mulliken population analysis [69] performed with the 6-31G* basis set on IAA [70].

Two different alignments were performed for each set of conformers (P and T): (a) electrostatic (E) and (b) steric–electrostatic (SE). In the former, the weights of the electrostatic and steric terms in the expression that is minimized during the alignment are equal, but because of the presence of the deprotonated carboxyl group, the electrostatic term for the carboxyl is about two orders of magnitude larger than the steric term. This produces an alignment in which the carboxyl oxygens are overlaid as close to each other as possible. In the SE alignment, the steric and electrostatic terms are more balanced, since we used a 25 times larger weight for the steric than for the electrostatic term.

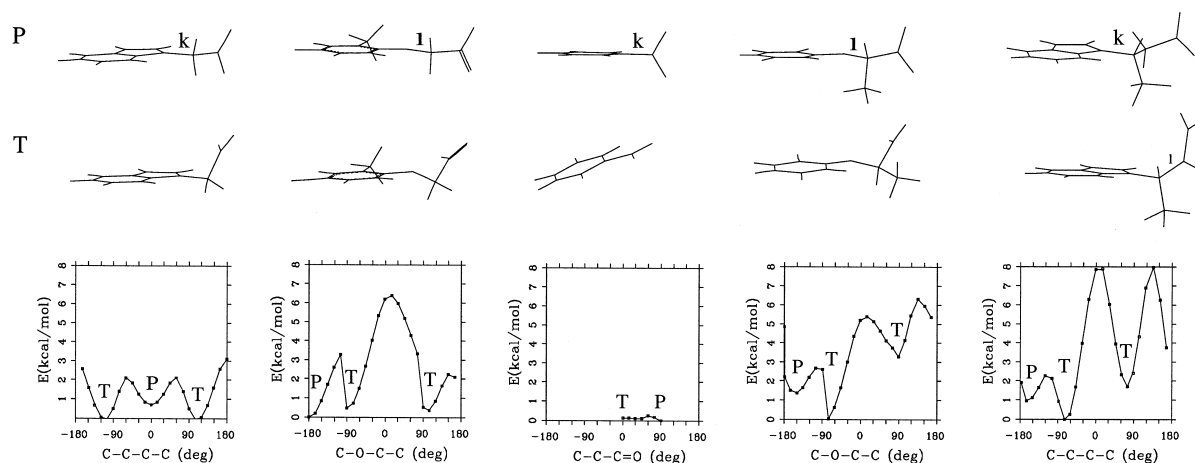


Figure 2. P (top) and T (bottom) conformations of (from left to right) IAA, 2-Me,4-Cl-PAA, BA, 2,5-Cl₂-PA₂PA (S) and TFIBA (R), and the 1D PES obtained by rotation about the bond labeled. The PESs were determined using the CFF91 force field in all cases except for BA, for which the PES was computed by quantum mechanical PM3 calculations [78]. Energies are given relative to that of the lowest energy conformer.

Alignment based on molecular interaction fields

Alignment using similarity indices (see below) was performed for two different sets of conformers: T and P. For this, the values of molecular interaction fields (see the following paragraph) calculated by the GRID program [71] at the molecular surface were replaced by Gaussians and similarity indices were optimized (see below).

Interaction energies

For both types of alignment, interaction energies with H₂O, NH₂⁺, CH₃, O and DRY [71] probes were calculated using the GRID program [71–75]. Maximum energy cutoffs between 7 and 30 kcal/mol were employed.

Interaction energies of compounds aligned using atomic properties

For compounds aligned using the SEAL program, interaction energies were calculated in a volume around the molecules. For each set of compounds (T-E, T-SE, P-E, P-SE), they were evaluated on identical grids, the size of which was chosen to include points within 4 Å of all atoms in the most extended (largest) molecule in the set. A dielectric constant of 4.0 was used over the whole grid. Computations were performed with both 1 Å and 2 Å grid spacings.

Interaction energies of compounds aligned using maximization of SIs

For the compounds aligned using this procedure, interaction energies were computed only on the molecular

probe accessible surfaces of the compounds to optimize the signal/noise ratio. The molecular surface was defined as an approximation of probe accessible surfaces [76]. It was constructed with about 2.0 Å distant surface points forming a triangular mesh with 150–200 points per compound. Two surfaces were constructed for each conformer: one with a 2.0 Å and one with a 2.5 Å radius probe. The interaction energies of the T and P conformers of each molecule with H₂O, NH₂⁺, CH₃ and O probes were calculated at these points using directive POSI in the GRID program [71]. The DRY probe was not used because the distribution of MIF for this probe in the molecular probe accessible surface is such that SI cannot be properly maximized.

The value of the molecular interaction field E^k at each point \mathbf{r}_k of the molecular surface was replaced by a Gaussian function: $E^k \exp(-\alpha(\mathbf{r}-\mathbf{r}_k)^2)$. Thus, the molecular interaction field of each molecule at point \mathbf{r} was given as:

$$E(\mathbf{r}) = \sum_k E^k \exp(-\alpha(\mathbf{r}-\mathbf{r}_k)^2) \quad (1)$$

The value of α was 1/4 Å⁻²; however, the results did not show significant dependence on this parameter.

Global minima locations

The positions of global minima for each set of compounds and for each probe were determined. The distribution of global minima was visualized with the INSIGHT program [64].

Similarity

For each pair of compounds (a,b), Carbo (C) [34,39] and Hodgkin (H) [40,41] similarity indices (SI) were calculated:

$$SI_C(a, b) = (\mathbf{E}_a, \mathbf{E}_b) / (\mathbf{E}_a^2 \mathbf{E}_b^2)^{1/2} \quad (2)$$

$$SI_H(a, b) = 2(\mathbf{E}_a, \mathbf{E}_b) / (\mathbf{E}_a^2 + \mathbf{E}_b^2) \quad (3)$$

where the scalar product $(\mathbf{E}_a, \mathbf{E}_b)$ is the sum of products of values of molecular interaction fields on grid points.

The similarity indices calculated above were used to determine class similarity indices (CSI) between classes:

$$CSI(i, j) = \sum_{i'} \sum_{j'} SI_x(i', j') / N_i N_j \quad (4)$$

where $x = H$ or C , $i' =$ compounds in class i , $j' =$ compounds in class j , $N_y =$ number of compounds in class y ($y=i, j$), or within one class:

$$CSI(i) = \sum_{i'} \sum_{i''} SI_x(i', i'') / N_i^2 \quad (5)$$

where i' and i'' are compounds in class i .

Although the H indices are more sensitive to the constant scaling factor than the C indices, the difference between them was insignificant for our problem, i.e. for the same probe, differences between the H and C class similarity indices $CSI(i)$ are of about the same magnitude as the standard deviations obtained for the single compound class similarity indices (see below) per class. C indices are systematically about 2% higher than H indices, but the relations between the classes are essentially indistinguishable for the two indices. Therefore, only the results for H indices are given.

The indices given above include a self-similarity term and when the similarity within a class is low and/or the number of pairs in the sum is small, this can lead to an artificially high CSI. For this reason, indices (CSI^*) from which self-similarity was excluded were calculated as well:

$$CSI^*(i) = \sum_{i'} \sum_{i' \neq i''} SI_x(i', i'') / (N_i(N_i - 1)) \quad (6)$$

with i and N as in Equation 5. The relation between these two indices is:

$$CSI(i) = CSI^*(i) + (1 - CSI^*(i)) / N_i \quad (7)$$

To determine the relative similarity between classes and different subsets of classes (two, three or more), for various probes, additive indices (ASI) were calculated:

$$ASI(i, \dots, n) =$$

$$\frac{\sum_{i'} \sum_{i' \neq i''} SI(i', i'')}{(N_i + \dots + N_n)(N_i + \dots + N_n - 1)} \quad (8)$$

where $i, \dots, n =$ classes, $N_i =$ the number of compounds in class i , and i' and i'' are compounds in the i, \dots, n classes.

In order to evaluate the goodness of classification of each compound, single compound tests were performed for H_2O , NH_2^+ , CH_3 and O probes for both 1 and 2 Å spacing grids. A single compound similarity index, SSI, was determined from the similarity of a single compound (i') to the other compounds (i'') in the same class (i), and to those in different classes of compounds (j).

$$SSI(i') = \sum_{i' \neq i''} SI(i', i'') / N_i \quad (9)$$

$$SSI_j(i') = \sum_{j'} SI(i', j') / N_j \quad (10)$$

Optimization of similarity indices for alignment

Molecules were aligned by optimizing the SIs for the molecular interaction fields calculated at the molecular probe accessible surface. The SI of a pair of compounds was defined as before (see Equations 2 and 3), but the scalar product of two molecular fields was given as an integral:

$$(\mathbf{E}_1 \mathbf{E}_2) = \int d^3 \mathbf{r} \mathbf{E}_1(\mathbf{r}) \mathbf{E}_2(\mathbf{r}), \quad (11)$$

instead of a sum over the grid points.

The SI defined in this way is an analytical function of the six rotational and translational degrees of freedom of two rigid molecules. Maximization of the SIs with respect to these coordinates was performed by the following procedure. Several orientations and displacements of molecules were generated randomly. Starting from each of these, maximization was performed first by conjugate gradient and then by Newton methods [77]. We found that, for our compounds, it is sufficient to generate 10 starting sets of coordinates to locate the global maximum of SI; a larger number of starting sets (up to 50) did not change the result.

Classification of compounds according to their similarity to 'kernels'

'Kernels' of the four initial classes of compounds were built to contain the best representatives of the classes

as regards their biological characteristics. The number of compounds was chosen to ‘cover’ the largest possible area in the multidimensional space of each class with the smallest number of compounds. Thus, the kernels are minimum representative sets of compounds. To check the predictive ability of the model, the similarity of the already classified compounds to each kernel was calculated. For this purpose MIFs determined with the GRID program [71] on the points in the molecular surface were used. The choice of the compounds in the kernels was iteratively optimized until satisfactory classification of the majority of compounds was achieved.

Kernels were also constructed in a similar manner for screening the activities of new compounds.

Results

Conformational analysis

According to the data available on the molecular conformation of IAA and its analogues and derivatives (alkylated and halogenated) extracted from their X-ray structures [22–24,29] and evaluated by *ab initio* SCF calculations [27,28], molecular mechanics and molecular dynamics simulations [23,24], there are rather small energy differences (less than 3 kcal/mol) between the planar and tilted conformations of auxins—derivatives of indole-3-acetic acid. Similarly, for the other compounds analyzed, the energy differences between P and T conformers are less than 5 kcal/mol. Such small energy differences could easily be compensated by solvation or binding to the receptor. All of the compounds analyzed have at least one barrier over which transition is feasible at room temperature. However, the shape of the PES can differ significantly for different compounds. This is shown in Figure 2 for rotation about the first or second bond, k or l, of the principal side chain of the compounds analyzed. For the IAA and PAA derivatives, the 1D-PES is approximately symmetric, i.e. there are two tilted conformers with similar energies and a transition from the extended P conformer to any of the T conformers or *vice versa* can occur easily. For PA2PA and 3-IBA derivatives, the T conformers differ in energy and transitions between the two T conformers and from the extended P conformer to the higher energy T conformer are less feasible. However, the IAA, PAA and PA2PA (R and S) derivatives (see Table 1) have varying biological activity and it is difficult to relate differences in the shape

of their potential energy surfaces to differences in biological activity. If the mechanism of action of auxins involves a conformational change from a binding to a modulation conformation as proposed by Kaethner [15], the energy barrier between the two conformers analyzed is such that all compounds would be expected to be able to undergo the necessary transition. Auxins cannot be distinguished from antiauxins or inactive compounds on the basis of the height of the energetic transition barrier between conformations.

Edgerton et al. [25] reported that the putative receptor binding conformation of indole-3-acetic acid and some other auxins has the plane of the carboxyl group orthogonal to the aromatic ring plane with the carboxyl oxygens positioned astride to the ring system. They, however, performed only molecular mechanics conformational analysis of compounds. According to our *ab initio* quantum mechanical calculations on IAA and 4-Cl-IAA [27,28], experience with the reliability of force fields [23,24,67], and the results of conformational analysis on the other auxins and their analogues performed in the present study, conformational analysis alone is insufficient to claim that any of these conformers is the sole binding conformation.

Molecular interaction fields

Some of the global energy minima determined from GRID calculations with a 1 Å spacing for five different probes are shown in Figure 3. Active and inactive compounds cannot be distinguished from analysis of the distribution of the energy minima, as they often overlap for active and inactive compounds. This is true for both SEAL and SI alignments, since the type of alignment does not significantly influence the positions of the MIF minima. However, there are some outlying energy minima. For example, those for NH_2^+ , H_2O and DRY probes with TFIBA (Table 1, **41**), a strong antiauxin, in the T-E, P-E and T-SE sets are far from the region in which the majority of the global minima are clustered. The same is true for the global minima obtained for the interaction of the CH_3 probe with 2-I-BA (**32**), 2,6-Cl₂-BA (**33**), 4-Cl-BA (**35**) and BA (**34**) in the T-SE set and with 4-Cl-PIBA (**38**) in the P-SE set. All except the last of these compounds are inactive compounds and are outliers because they are smaller than most of the compounds analyzed. However, not all compounds with large deviations from the average size have consistently outlying minima.

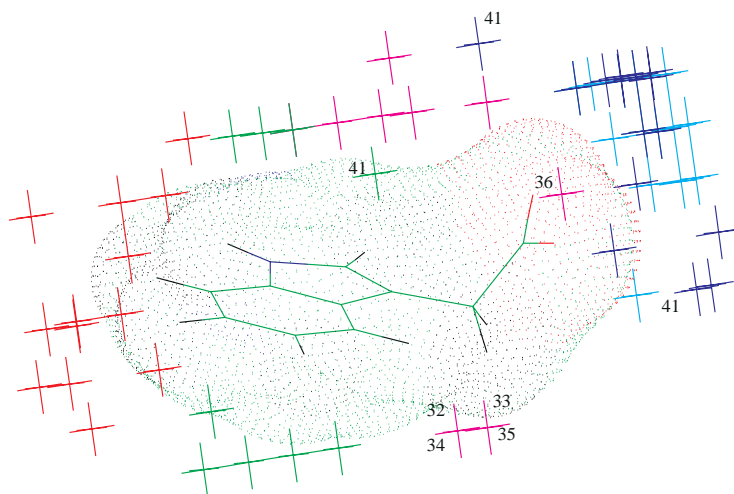


Figure 3. Positions of global energy minima for five probes determined with the GRID program for the T-SE set of conformers are displayed around the tilted (T) IAA conformer (its 2 Å probe accessible surface is represented by dots). Visually similar distributions of global energy minima were also obtained for the other three sets. Key: blue: H₂O, cyan: NH₂⁺; pink: CH₃; red: O; green: DRY probe. Minima far from the most populated regions are labeled by compound code number (Table 1).

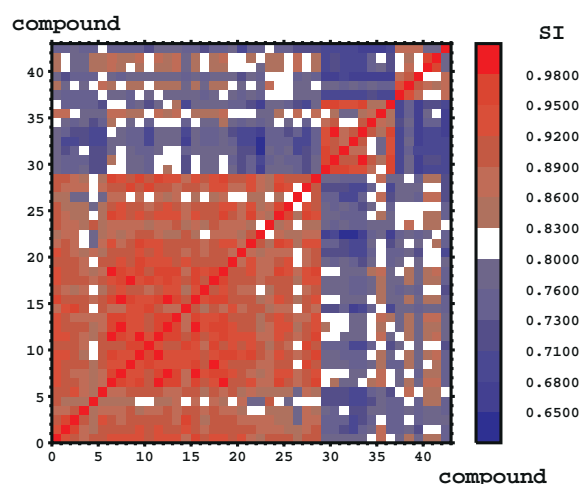


Figure 4. Hodgkin similarity indices for the molecular interaction fields in the T-E set determined for the CH₃ probe. Each square corresponds to the similarity between two compounds with self-similarity on the diagonal. Compounds are ordered as in Table 1. The identifier codes (see Table 1) are given on the axes; for the compounds with two stereo isomers only the S-isomer is used in the similarity analysis. The values of the similarity indices are given by the color according to the spectrum. Note that similarity is higher between compounds in the same class.

Initial classification

As stated above, from inspection of the PESs and the positions of the global minima in the MIFs alone we cannot deduce a compound's activity. On the other hand, molecular interaction field vectors are more

informative. Inspection of the 46 × 46 SI matrix (Equations 2 and 3) (for the first 43 compounds including three stereo isomers in Table 1) enables us to roughly distinguish active compounds from inactive ones (see e.g. Figure 4).

Defining classes: CSIs

Compounds were divided into classes according to their measured biological activities and the similarity between their molecular interaction fields. In all sets (P-E, P-SE, T-E, T-SE), for all the probes utilized to determine molecular interaction fields on the 1 Å spacing grid, the similarity between compounds in a class (when self-similarity is included in the CSI calculation) was higher than the similarity between compounds in different classes: CSI(i) > CSI(i,j), (j ≠ i) (see Figure 5 for the results on the T-SE set). The only exception was class 4 (antiauxins) in the P-SE set for the DRY probe. According to the CSIs calculated for this probe, compounds in class 4 were on average more similar to the compounds in class 1 (auxins) than to the compounds in class 4. This was true both for Hodgkin and Carbo indices.

The results obtained with a 2 Å grid spacing were quite similar to those obtained with a 1 Å grid spacing. However, for the T-SE and P-SE sets, the classes were better defined with a 1 Å grid spacing. In contrast, for the P-E set, the classes are better defined with a 2 Å grid spacing in the sense that classes 2 and 4 were better distinguished from the other classes. The CSIs

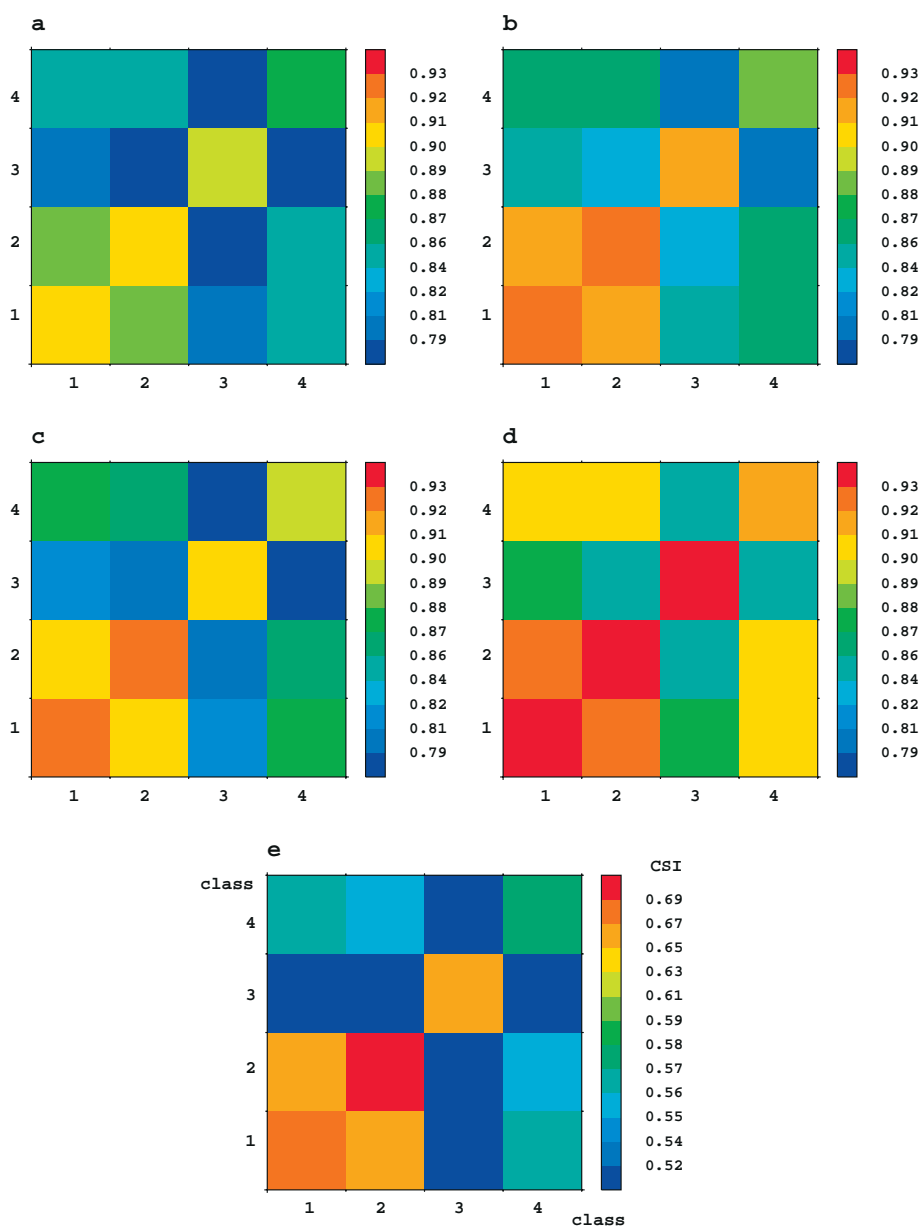


Figure 5. Class similarity indices (CSI) determined for each probe for the T-SE set: (a) H₂O; (b) NH₂⁺; (c) CH₃; (d) O; (e) DRY. Each square corresponds to the similarity between two classes with self-similarity on the diagonal. The class numbers are given on the axes. The values of the class similarity indices are given by the color according to the spectrum (note that the scale is different in (e)).

provide support for the division of the compounds into the four chosen classes. Classes 1 and 3 were also well defined when class similarity indices CSI* (Equation 6) that exclude self-similarity were utilized, but the separation of the other classes was not as clear as above.

Testing classification: SSIs, re-evaluation of the bioassay data and new classification

SSIs (Equations 9 and 10) were calculated in order to evaluate the classification of each compound, i.e. to identify the compounds which were the most dissimilar to the compounds in the same class, and possibly more similar to compounds in other classes.

For more than 75% of the compounds the largest SSIs were determined for the compounds from the same class, $SSI(i') > SSI_j(i')$, i.e. the initial classification was successful for the majority of molecules. For some of the compounds that, according to this analysis, should be classified differently (e.g.: 7-Cl-IAA (Table 1, **25**), 5,7-Cl₂-IAA (**28**), 2-NAA (**29**)), there is a discrepancy between different biological activity measurements. The contradictory experimental evidence in the literature on the biological activity of some auxins makes their classification particularly complicated. For example, Hatano and co-workers [43] found that 6,7-Cl₂-IAA (**22**) is a very active auxin in *Avena* while, according to Böttger et al. [57], it is almost inactive in this plant. For some other halogenated derivatives of IAA, i.e. 5,7-Cl₂-IAA, 4,7-Cl₂-IAA (**26**) and 7-Cl-IAA, diverse biological activities were measured [29,43,46,49,57,63] as well. For 3-IPA (**27**), Ray et al. [42] measured strong binding with inhibitory behaviour at low concentrations and auxin characteristics at higher concentrations ($> 10^{-5}$ M). According to Katayama et al. [45], 3-IPA (**27**) is a weakly active auxin over a wide range of concentrations ($\approx 10^{-7}$ – 10^{-4} M). Species-specific properties of the auxin receptors may explain some of these differences. Another possible explanation is given by differences in the conditions under which the experiments were performed. The changes in activity upon variation of auxin concentration may be related to the tissue sensitivity to growth substances which may depend on receptor-hormone binding affinity. Initially, we treated both 7-Cl-IAA and 6,7-Cl₂-IAA as moderately active auxins (belonging to class 1). From single compound analysis (i.e. according to SSIs computed from Equations 9 and 10), it seems that this was a good choice for 6,7-Cl₂-IAA since 12 out of the 16 molecular interaction fields calculated for it (in the four sets T-E, T-SE, P-E, P-SE, for four different probes, H₂O, NH₂⁺, CH₃, O) were more similar to the average interaction energy field of class 1 than to those of other classes. However, for 7-Cl-IAA, the corresponding proportion is less than 50%, and it turned out to be more similar to compounds in class 2 than in class 1. Conversely, R(D)-2,5-Me₂-PA2PA (**24**) was initially put in class 2, but, in accord with Ray's measurements [42], its interaction field turned out to be more similar to those of compounds in class 1. In further analysis, we considered 7-Cl-IAA and R(D)-2,5-Me₂-PA2PA as belonging to classes 2 and 1, respectively.

Ray et al. [42] found that 2-NAA (**29**) binds strongly to ABP1 and has weak inhibitory character-

istics, but according to Hansen's measurements on *Avena* coleoptile cylinder [59] and pea stem assays, it is a weak auxin. Initially, 2-NAA was put in class 4, but later on, based on the experimental data and the similarity analysis, we transferred it to class 2. These are examples where similarity analysis assisted in resolving ambiguities in the literature and the proper classification of compounds. However, in subsequent analysis, compounds were left in the initial class if similarity analysis suggested a different classification with no evidence for it in the literature; for example, according to similarity analysis 3-IBA (**42**) belongs to class 2, but was kept in class 4 [45].

Refinement of the classification model

Alignment of compounds by SI maximization

By representing molecular interaction fields at points on molecular probe accessible surfaces by Gaussians, it is possible to align molecules by optimizing their SIs. Such an alignment has advantages relative to those performed by the SEAL program in the sense that no arbitrary parameters, e.g. weights for different terms in the expression that is optimized by the SEAL program, are used. Also data handling is faster because there is no need to switch between so many various programs as when using SEAL. The average differences between the resulting SEAL and SI alignments are small; average rms deviations between the 46 molecules aligned in the two different ways are about 0.8 Å and SI improvements about 2%. However, for some compounds, mostly those from classes 3 and 4, the rms deviation can be as great as 4 Å and the SI improvement as great as 15%.

Evaluation of the final model

For the P and T sets of conformations aligned by SI maximization, using molecular interaction fields for the NH₂⁺ probe, the ratios of CSI*s were calculated for H₂O, NH₂⁺, CH₃ and O probes and the results are presented in Table 2. The ratios can be better understood if they are analyzed together with relative normalized additive similarity indices (Δ ASIs, Equation 12) (Figure 6). From Figure 6, it is obvious that the similarity within the individual classes 1, 2 and 3 is greater in the T than the P set. However, in both sets it is much above the similarity within the whole set of compounds. Class 2 consists of only five compounds and thus has a low statistical weight. The similarity within class 4 (antiauxins) is very low in both sets of conformations, i.e. the molecular interaction fields

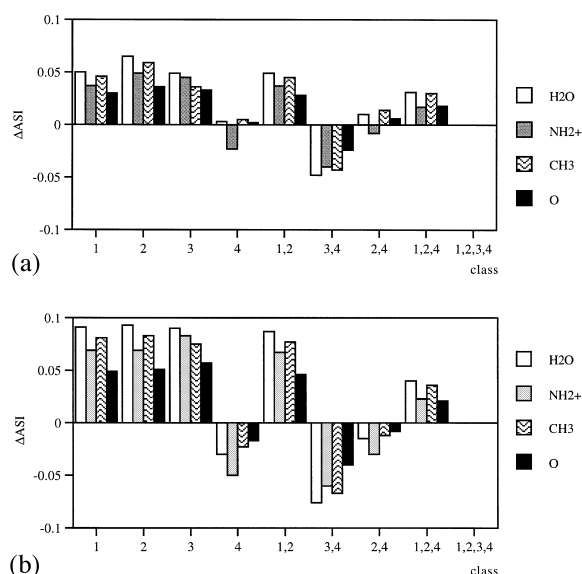


Figure 6. Relative normalized additive similarity indices: $\Delta ASI = A(i, \dots, n) / A(1, 2, 3, 4) - 1$ where i, \dots, n are the classes for which additive similarity is calculated. Indices are given for P (upper plot) and T (lower plot) sets of conformers. Compounds were aligned by optimizing the SI for the NH_2^+ probe, using a 2.5 Å radius probe accessible surface.

of the compounds in this class are not very similar. However, the values of the 3,3/3,4 and 4,4/4,3 CSI^* ratios are high (Table 2) and the ASI when classes 3 and 4 are put together is always small ($\Delta ASI(3,4) < 0$, see Figure 6). So, class 4 is well distinguished from class 3. This means that compounds with antiauxin characteristics are not similar to the compounds that are inactive. Similarity within the set of compounds consisting of classes 1, 2 and 4 is lower than within classes 1 and 2 themselves, i.e. within the set of similar compounds, compounds from class 4 are the most different. These data support the existence of class 4 as a separate class. We expect that compounds with interaction energy fields similar to those of the compounds in class 4 have antiauxin characteristics.

Screening of compounds by comparison to class kernels

The analysis above shows that the classes are distinguishable (Figure 5), i.e. every class appeared to be more similar to itself than to any other. This is the first condition that must be fulfilled for a model to be predictive. The next step is to build a model that can predict that class any given compound belongs to. Therefore, we redefined the classes by their minimum representative set or kernel of compounds, developed

Table 2. Ratios of class similarity indices (CSI_{ii}^*/CSI_{ij}^*)^a calculated for the final classification of the first 46 compounds in Table 1 (43 compounds including 3 stereo isomers)

Classes ^a	Probe			
	H ₂ O	NH ₂ ⁺	CH ₃	O
1,1/1,2	1.01	1.01	1.02	1.01
	1.00	1.00	1.00	1.00
1,1/1,3	1.19	1.12	1.17	1.10
	1.09	1.05	1.10	1.06
1,1/1,4	1.14	1.14	1.13	1.08
	1.08	1.07	1.06	1.05
2,2/2,1	1.01	1.01	1.02	1.01
	1.01	1.00	1.01	1.00
2,2/2,3	1.21	1.12	1.18	1.11
	1.12	1.05	1.09	1.06
2,2/2,4	1.13	1.12	1.12	1.07
	1.09	1.07	1.06	1.03
3,3/3,1	1.19	1.14	1.16	1.11
	1.10	1.07	1.11	1.07
3,3/3,2	1.21	1.14	1.17	1.11
	1.10	1.06	1.10	1.07
3,3/3,4	1.31	1.24	1.27	1.16
	1.18	1.13	1.16	1.11
4,4/4,1	1.01	1.00	1.01	1.00
	1.00	0.99	1.00	1.00
4,4/4,2	1.00	1.01	1.01	1.00
	0.99	0.98	1.00	0.99
4,4/4,3	1.16	1.10	1.16	1.08
	1.08	1.01	1.08	1.05

Ratios were determined in T (upper value) and P (lower value) sets. Compounds were aligned by optimizing the SI for the NH_2^+ probe molecular interaction field on 2.5 Å radius probe accessible surfaces. The standard deviation of single compound similarity to any class for all compounds is about 2–4%.

^a The classes given correspond to the subscripts in the following expression of the ratio: (CSI_{ii}^*/CSI_{ij}^*).

a formalism to describe the similarity of a given compound to this kernel (given in Table 1), and tested its ability to properly classify any given compound on the basis of its molecular interaction fields. First, we checked the model on the compounds already classified. In the T set, most of the compounds from classes 1 and 3 were properly classified. With the NH_2^+ probe, all compounds in class 1 were properly classified except 7-F-IAA (Table 1, **19**), which was put in class 2 (Figure 7). This compound was put in class 2 by the O probe as well. 2,3,4-Cl₃-PAA (**15**) was the only com-

pound from class 1 that was put in another class three times: by the NH_2^+ and CH_3 probes in class 2 and by the O probe in class 4. It is interesting that this compound is active on pea [50,51] (there are no activity measurements for this compound on maize and *Avena*) like 5,7- Cl_2 -IAA (**28**) and 7- Cl -IAA (**25**) [63], which belong to class 2. This indicates that the auxin receptor in pea may be different from those in *Avena* and maize. With the O probe, S(L)-2,4- Cl_2 -PA2PA (**6**) and 6,7- Cl_2 -IAA (**22**) were also put in class 4, although they were properly classified by the other probes. From class 2, the compounds 5,7- Cl_2 -IAA (**28**) and 2-NAA (**29**) were properly classified only once, by the O and H_2O probe respectively, otherwise they were put in class 1. However, their similarity to the kernels of classes 1 and 2 does not differ significantly. All compounds from class 3 were properly classified. Two of the eight compounds from class 4 were not properly classified by any probe: both isomers of 3-IBA (**42**, Table 1) according to this screening belong to class 2. The other compounds from this class were classified as expected by at least two probes. S(D)-3F₃-IBA (**41**) was put in class 1 by the NH_2^+ probe (R(L)-3F₃-IBA in class 3) and in class 3 by the O probe, and IIBA (**39**) was classified in class 1 by the CH_3 and O probes.

To make a robust screen for whether a compound has auxin activity, i.e. is a member of classes 1 or 2 or not, SSIs were computed for each compound against an auxin kernel consisting of the compounds in the kernels of classes 1 and 2, and two more compounds from class 1, see Figure 8. Within the T set of conformers it screens all inactive compounds and the majority of antiauxins from auxins.

Classification of new compounds

An attempt was made to classify additional compounds (see Table 1, compounds **44–53**) according to their similarities to the auxin kernel defined in the previous section. With the combined class 1 and class 2 kernels, the following compounds were screened out as compounds not belonging to auxins (Figure 8): 3,4,5- I_3 -BA (**44**), which is according to Ray's measurements [42] a strong inhibitor; 3,4- Cl_2 -BA (**45**), for which Ray et al. [42] determined a low binding constant and inhibitory characteristics at high ($> 10^{-4}$ M) concentrations; 2,3,5- Cl_3 -BA (**48**), declared in the literature [60] as an inactive compound; 2,4,6- Cl_3 -PAA (**49**), which is inactive according to Mür and Hansch [55] and Fawcett et al. [51]; 2,3,5- I_3 -BA (**50**), which binds strongly [42], at low concentrations ($\approx 10^{-5}$ M)

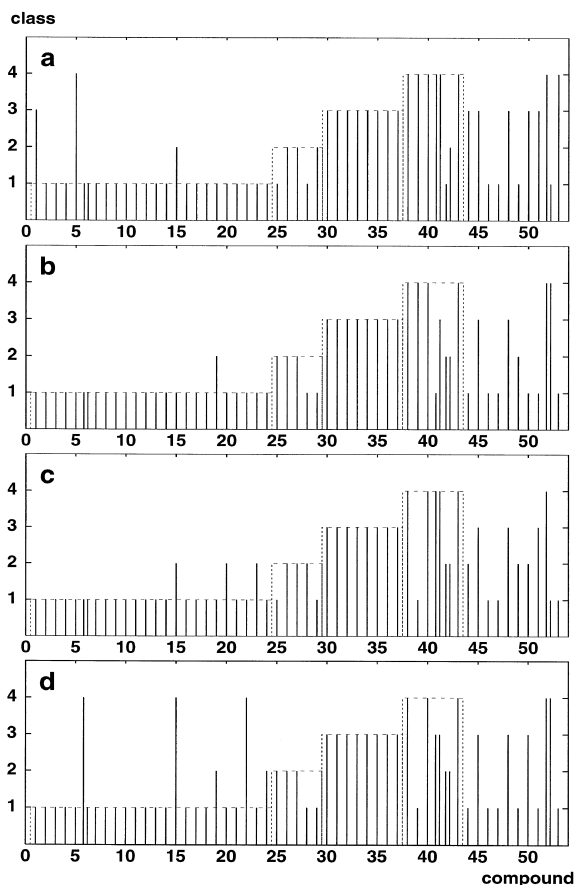


Figure 7. Screening of compounds by their similarity to kernel compounds. Compound codes (as in Table 1, the first row) are given on the x axes and the lines indicate to which class each compound belongs, as shown on the y axis, according to the similarity analysis with the (a) H_2O ; (b) NH_2^+ ; (c) CH_3 and (d) O probes. Stereo isomers are represented with two close lines above a code number (Table 1, the first row). Compounds previously classified are enclosed in dashed boxes; class 1: compounds **1–24**; class 2: compounds **25–29**; class 3: compounds **30–37**; class 4: compounds **38–43**.

acting as an auxin and at high ($> 10^{-4}$ M) concentrations as an inhibitor, with Hatano et al. [44] reporting that it is an antiauxin inducing upcurling of roots; PAA (**51**), which according to Fawcett et al. [51] and Mür and Hansch [55] is an inactive compound, although Ray et al. measured low binding to ABP1 [42], and S-3,5- Cl_2 -PA2PA (**52**), for which there are no binding measurements, but which is declared to possess no auxin characteristics [20,62].

Compounds 2-Me-IAA (**46**), 2,5-Me₂-PAA (**47**) and S(L)-2,5-Me₂-PA2PA (**53**) seem to belong to weak auxins according to the similarity analysis. Klämbt [48] measured the binding of 2-Me-IAA to ABP1, and

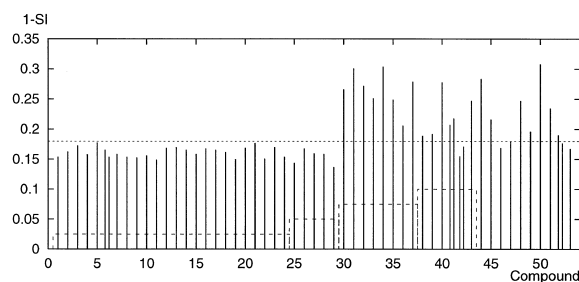


Figure 8. Screening of compounds by their similarity to an auxin kernel, consisting of class 1 and class 2 kernels and two additional compounds from class 1: **5** and **23**. The T set of conformers and the NH_2^+ probe are utilized. Compound codes are given on the x axis and the lines correspond to the values of 1-SSI(i) (y axis) calculated for each compound against this kernel. Compounds previously classified are enclosed in dashed boxes; class 1: compounds **1–24**; class 2: compounds **25–29**; class 3: compounds **30–37**; class 4: compounds **38–43**.

found that it is very low. However, according to some other measurements on *Avena* coleoptiles and pea stem assays [14,55] it is a weak auxin. According to Ray et al. [42], 2,5-Me₂-PAA (**47**) and S(L)-2,5-Me₂-PA2PA (**53**) bind moderately, but they have inhibitory characteristics in a narrow range of concentrations ($< 10^{-4}$ M). Mür and Hansch [55] found that 2,5-Me₂-PAA is a weak auxin. The final classification of these compounds, given in Table 1, is achieved taking into account both similarity analysis and biological data available. Some authors [62] found that PAA and PA2PA derivatives with the same substituents have similar biological activity. According to the screening and the biological data, both 2,5-Me₂-PAA and S(L)-2,5-Me₂-PA2PA belong to class 2.

Discussion

As already mentioned in the Introduction, several theories address the mechanism by which auxins induce a biological response. In the conformational change theory, Kaethner [15] proposed that auxin can adopt a planar recognition conformation and that on binding to the receptor, the molecule changes to the modulation, tilted conformation (the side chain with the carboxyl group is perpendicular to the aromatic plane). On the other hand, in the ‘single conformation’ theories [14,16,18,19] the recognition conformation is also the modulation conformation.

In our interaction similarity study, the classes are better distinguished when the T conformations of compounds are used. This suggests that the tilted

conformation is the active one, and, in single conformation theories, this is the same as the recognition conformation. However, if we presume that the conformational change theory [15,16] is correct, we can speculate, from the results obtained, that the auxins bind in a planar conformation (for the compounds from class 1 this is the P conformer) and then change to the active-tilted one (T conformer). In the planar conformation, antiauxins (class 4: P set) are more similar to auxins (class 1) than in the tilted conformation ($\text{CSI}_{1,1}^*/\text{CSI}_{1,4}^*$ is higher in the T than in the P set, and the same is true, with much lower accuracy, for the 4,4/4,1 ratio), so binding should be strong but activation poor. Further support for a conformational change from the P to the T conformation is given by the low computed energy barriers between the two conformers.

Conclusions

The classification of about 50 auxins and their analogues into four classes, according to their interaction properties, has been achieved. In the final model, compounds are aligned by optimizing their MIFs. This alignment procedure is physically justified because molecules are aligned and distinguished on the basis of their interaction with selected functional groups that could correspond to those in the receptor. This procedure also resulted in a slight improvement in the final model compared to performing a more conventional alignment according to atomic properties. When T conformers are used, the model enables auxins to be distinguished from antiauxins and inactive compounds. Although the similarity analysis presented cannot provide a definitive ligand binding mechanism, better differentiation of classes when T conformers are used suggests that the T conformation might be the active one. The knowledge gained in this analysis can provide a guideline for new bioassays required to address the contradictions in the literature regarding auxin activities of a number of compounds.

Acknowledgements

S.T. is the recipient of a postdoctoral fellowship from the Alexander von Humboldt Foundation. This work was supported in part by German-Croatian WTZ, Project KRO-001-95. We are grateful to Prof. D.

Klämbt for discussions and to Dr. I. Shrivastava for reading of the manuscript.

References

- Davies, P.J., *Plant Hormones and Their Role in Plant Growth and Development*, Martinus Nijhoff, Dordrecht, The Netherlands, 1987.
- Thimann, K.V., *Hormone Action in the Whole Life of Plants*, The University of Massachusetts Press, Amherst, MA, U.S.A., 1977.
- Palme, K.J., *Plant Growth Regul.*, 12 (1993) 171.
- Klämbt, D., *Plant Mol. Biol.*, 14 (1990) 1045.
- Jones, A.M., *Physiol. Plant.*, 80 (1990) 154.
- Jones, A.M. and Prasad, P.V., *BioEssays*, 14 (1992) 43.
- Venis, M.A. and Napier, M., *Crit. Rev. Plant Sci.*, 14 (1995) 27.
- Tian, H., Klämbt, D. and Jones, A.M., *J. Biol. Chem.*, 270 (1995) 26962.
- Löbber, M. and Klämbt, D., *J. Biol. Chem.*, 260 (1985) 9848.
- Shimomura, S., Sotobayashi, S., Futai, M. and Fukui, T., *J. Biochem.*, 99 (1986) 1513.
- Inohara, N., Shimomura, S., Fukui, T. and Futai, M., *Proc. Natl. Acad. Sci. USA*, 86 (1989) 3564.
- Napier, R.M., Venis, M.A., Bolton, M.A., Richardson, L.I. and Butcher, G.W., *Planta*, 176 (1988) 519.
- Veldstra, H., *Enzymologia*, 11 (1944) 97.
- Porter, W.L. and Thimann, K.V., *Phytochemistry*, 4 (1965) 229.
- Kaethner, J.M., *Nature*, 267 (1977) 19.
- Farrimond, J.A., Elliott, M.C. and Clark, D.W., *Nature*, 274 (1978) 401.
- Lehmann, P.A.F., *Chem.-Biol. Interact.*, 20 (1978) 239.
- Rakhaminova, A.B., Khavkin, E.E. and Yaguzhinskii, L.S., *Biokhimiya*, 43 (1978) 806.
- Katekar, G.F., *Phytochemistry*, 18 (1979) 223.
- Pattabhi, V., *Curr. Sci.*, 59 (1990) 1228.
- Bures, M.G., Black-Schaefer, C. and Gardner, G., *J. Comput.-Aided Mol. Design*, 5 (1991) 323.
- Kojić-Prodić, B., Nigović, B., Tomić, S., Ilić, N., Magnus, V., Konjević, R., Giba, Z. and Duax, W.L., *Acta Crystallogr.*, B47 (1991) 1010.
- Nigović, B., Kojić-Prodić, B., Antolić, S., Tomić, S., Puntarec, V. and Cohen, J.D., *Acta Crystallogr.*, B52 (1996) 332.
- Antolić, S., Kojić-Prodić, B., Tomić, S., Nigović, B., Magnus, V. and Cohen, J.D., *Acta Crystallogr.*, B52 (1996) 651.
- Edgerton, M.D., Tropsha, A. and Jones, A.M., *Phytochemistry*, 35 (1994) 1111.
- Beale, M.H. and Sponsel, J., *Plant Growth Regul.*, 12 (1996) 227.
- Ramek, M., Tomić, S. and Kojić-Prodić, B., *Int. J. Quant. Chem., Quant. Biol. Symp.*, 22 (1995) 75.
- Ramek, M., Tomić, S. and Kojić-Prodić, B., *Int. J. Quant. Chem.*, 60 (1996) 1727.
- Lutz, B.T.G., Van der Windt, E., Kanters, J., Klämbt, D., Kojić-Prodić, B. and Ramek, M., *J. Mol. Struct.*, 382 (1996) 177.
- Wade, R.C., In Kubinyi, H. (Ed.) *3D QSAR in Drug Design: Theory, Methods and Applications*, ESCOM, Leiden, The Netherlands, 1993, pp. 486–505.
- Good, A.C., In Dean, P.M. (Ed.) *Molecular Similarity in Drug Design*, Blackie Academic & Professional, London, U.K., 1995, pp. 1–23.
- Burt, C. and Richards, G., *J. Comput. Chem.*, 11 (1990) 1139.
- Richard, A.M., *J. Comput. Chem.*, 12 (1991) 959.
- Carbo, R., Arnau, M. and Leyda, L., *Int. J. Quant. Chem.*, 17 (1980) 1185.
- Klebe, G., Abraham, U. and Mietzner, T., *J. Med. Chem.*, 37 (1994) 4130.
- Cramer III, R.D., De Priest, S.A., Patterson, D.E. and Hecht, P., In Kubinyi, H. (Ed.) *3D QSAR in Drug Design: Theory, Methods and Applications*, ESCOM, Leiden, The Netherlands, 1993, pp. 443–485.
- Kearsley, S.K. and Smith, G.M., *Tetrahedron Comput. Methodol.*, 3 (1990) 615.
- Bagdassarian, C.K., Schramm, V.L. and Schwartz, S.D., *J. Am. Chem. Soc.*, 118 (1996) 8825.
- Carbo, R. and Calabuig, B., *Int. J. Quant. Chem.*, 42 (1992) 1681.
- Hodgkin, E.E. and Richards, W.G., *Int. J. Quant. Chem., Quant. Biol. Symp.*, 14 (1987) 105.
- Good, E.E., Hodgkin, E.E. and Richards, W.G., *J. Chem. Inf. Comput. Sci.*, 32 (1992) 188.
- Ray, P.M., Dohrmann, U. and Hartel, R., *Plant Physiol.*, 60 (1977) 585.
- Hatano, T., Katayama, M. and Marumo, S., *Experientia*, 43 (1987) 1237.
- Hatano, T., Kato, Y., Katayama, M. and Marumo, S., *Experientia*, 45 (1989) 400.
- Katayama, M., Kato, Y., Kimoto, H. and Fuji, S., *Experientia*, 51 (1995) 721.
- Katekar, G.F. and Geissler, A.E., *Phytochemistry*, 21 (1982) 257.
- Katekar, G.F. and Geissler, A.E., *Phytochemistry*, 22 (1983) 27.
- Rescher, U., Walther, A., Schiebl, C. and Klämbt, D., *J. Plant Growth Regul.*, 15 (1996) 1.
- Reinecke, D.M., Ozga, J.A. and Magnus, V., *Phytochemistry*, 40 (1995) 1361.
- Wain, R.L. and Wightman, F., *Ann. Appl. Biol.*, 40 (1953) 244.
- Fawcett, C.H., Wain, R.L. and Wightman, F., *Ann. Appl. Biol.*, 43 (1955) 342.
- Veldstra, H. and Van der Westeringh, C., *Recl. Trav. Chim. Pays-Bas*, 70 (1951) 1113.
- Brustrom, H., *Physiol. Plant.*, 3 (1950) 277.
- Nitsch, J.P. and Nitsch, C., *Plant Physiol.*, 3 (1956) 94.
- Mür, R.M. and Hansch, C., *Physiol. Plant.*, 28 (1953) 218.
- Stenlid, G. and Engvild, K.C., *Physiol. Plant.*, 70 (1987) 109.
- Böttger, M., Engvild, K.C. and Soll, H., *Planta*, 140 (1978) 89.
- Toothill, J.R., Wain, R.L. and Wightman, F., *Ann. Appl. Biol.*, 44 (1956) 547.
- Hansen, B., *I. Bot. Nat.*, (1954) 230.
- Veldstra, H., *Recl. Trav. Chim. Pays-Bas*, 71 (1952) 15.
- Pybus, M.F., Wain, R.L. and Wightman, F., *Nature*, 182 (1958) 1094.
- Smith, G., Kennard, C.H.L. and White, A.H., *Acta Crystallogr.*, B34 (1978) 2885.
- Hoffmann, A.L., Fox, S.W. and Bullock, M.W., *J. Biol. Chem.*, 196 (1952) 437.
- INSIGHT, v. 95, Biosym Technologies, San Diego, CA, U.S.A., 1995.

65. DISCOVER, v. 2.97, Biosym Technologies, San Diego, CA, U.S.A., 1995.
66. Maple, J.R., Thacher, T.S., Dinur, U. and Hagler, A.T., Chem. Design Autom. News, 5(9) (1990) 5.
67. Gundertofte, K., Liljefors, T., Norrby, P.O. and Pettersson, I., J. Comput. Chem., 17 (1996) 429.
68. Dauber-Osguthorpe, P., Roberts, V.A., Osguthorpe, D.J., Wolff, J., Genest, M. and Hagler, A.T., Proteins Struct. Funct. Genet., 4 (1988) 31.
69. Mulliken, R.S., J. Chem. Phys., 23 (1955) 1833.
70. Tomić, S., Ph.D. Thesis, University of Zagreb, Zagreb, Croatia, 1993.
71. GRID user manual, edition 14, Molecular Discovery Ltd., Oxford, U.K.
72. Goodford, P.J., J. Med. Chem., 28 (1985) 849.
73. Boobbyer, D.N.A., Goodford, P.J., McWhinnie, P.M. and Wade, R.C., J. Med. Chem., 32 (1989) 1083.
74. Wade, R.C., Clark, K.J. and Goodford, P.J., J. Med. Chem., 36 (1993) 140.
75. Wade, R.C. and Goodford, P.J., J. Med. Chem., 36 (1993) 148.
76. Gabdoulline, R.R. and Wade, R.C., J. Mol. Graph., 14 (1996) 341.
77. Korn, G.A. and Korn, T.M., Mathematical Handbook for Scientists and Engineers, McGraw-Hill, New York, NY, U.S.A., 1961.
78. Stewart, J.J.P., J. Comput. Chem., 10 (1989) 209.
79. Tomić, S., Ramek, M. and Kojić-Prodić, B., Croat. Chem. Acta, (1998) in press.